Iranian Journal of Mathematical Chemistry

IJMC

DOI: 10.22052/IJMC.2025.257438.2053
Vol. 17, No. 1, 2026, pp. 95-112
Research Paper

Utilizing General Lagrange Scaling Functions for Two Classes of Fractional Optimal Control Problems

Sedigheh Sabermahani[1], Yadollah Ordokhani[2*] and Parisa Rahimkhani[3]

[1]Department of Mathematics Education, Farhangian University, P.O. Box 14665-889, Tehran, Iran
[2]Department of Mathematics, Faculty of Mathematical Sciences, Alzahra University, Tehran, Iran
[3]Faculty of Science, Mahallat Institute of Higher Education, Mahallat, Iran

Keywords:

General Lagrange scaling function,
General Riemann-Liouville fractional integration operational matrix,
General delay operational matrix

AMS Subject Classification (2020):

26A33; 35R11

Article History:

Received: 17 August 2025
Accepted: 15 November 2025

Abstract

This manuscript examines two categories of fractional optimal control problems (FOCPs) with fractional system and delay fractional system constraints. This scheme is based on the general Lagrange scaling functions (GLSFs), which can generate both orthogonal and non-orthogonal scaling functions by selecting different Lagrange nodes. Notably, the method is designed to be applied without initially choosing specific Lagrange nodes; instead, we leverage the potential advantages of GLSFs to develop new methods by considering various Lagrange nodes. Additionally, a general Riemann-Liouville fractional integration operational matrix (GR-LOP) and a general delay operational matrix (GDOP) are proposed for the considered functions. Next, by combining these operational matrices and the Gauss-Legendre integration method, we transform the original problems into systems of algebraic equations. To demonstrate the effectiveness of the proposed GLSF method, five numerical examples are provided.

1 Introduction

Fractional calculus focuses on extending the concepts of integral and differentiation to non-integer orders. Fractional calculus has found numerous applications in controlling complex dynamic systems, processing images, analyzing signals, studying quantum mechanics, and managing operations in the oil industry, as well as in biomedical, engineering, biological pattern analysis, and financial economics [1–8]. Due to the numerous applications of fractional calculus and its appearance in various types of existing equations and problems, numerous studies

*Corresponding author
E-mail addresses: s.saber@cfu.ac.ir (S. Sabermahani), ordokhani@alzahra.ac.ir (Y. Ordokhani), p.rahimkhani@mahallat.ac.ir (P. Rahimkhani)
Academic Editor: Abbas Saadatmandi

have been conducted on fractional operators, and various numerical methods have been introduced for the approximate solution of these problems. For example, the authors in [9] studied some generalized fractional integration. The variable-order fractional differential and integro-differential equations were solved numerically in [10, 11]. The Pell wavelet-optimization method was presented to solve two classes of fractional partial differential equations [12]. A certain fractional kinetic equation was investigated in [13]. Zhang et al. [14] proposed a general solution for impulsive fractional differential equations. The time-space fractional Schröding equations were solved by a matrix transformation scheme in [15]. Some techniques have been suggested in the field of fractional optimal control theory to computationally approximate fractional models. In this manuscript, we provide an overview of some of these methods. Heydari and Razzaghi [16] introduced extended Chebyshev cardinal wavelets for addressing delay optimal control problems with a dynamical system incorporating fractional derivatives. Salati et al. [17] introduced three direct techniques utilizing some fractional integral formulas for solving FOCPs. Ashpazzadeh et al. [18] designed a numerical strategy for addressing FOCPs with inequality constraints utilizing biorthogonal multiwavelets. Marzban and Malakoutikhah [19] employed a combination of block-pulse functions and orthonormal Taylor polynomials to tackle fractional delay optimal control problems (FDOCPs). Authors of [20] introduced a computational approach for addressing FOCPs by utilizing the Hermite scaling functions. Heydari [21] employed a method based on shifted Chebyshev polynomials for 2D optimal control problems. Mittag-Leffler wavelets have been used to solve FOCPs by proposing a Riemann–Liouville fractional integral operator [22]. Hassani et al. developed the generalized Bernoulli polynomial method for solving nonlinear one and two-dimensional FOCPs [23, 24]. 2D nonlinear variable-order FOCPs were solved in [25]. In addition, this class of problems was solved numerically by the generalized Bessel polynomials [26]. A hybrid technique was designed in [27] to find a solution to the mentioned problems. We recommend that the reader study the related works [28–32].

1.1 Applications in chemistry

Recently, FOCP, especially when combined with time delays, has become a powerful tool across engineering, physics, chemistry, and biological systems-for example, enabling precise trajectory optimization in fractional-order systems with delays. Motivated by the successful application of fractional calculus in many different situations, some researchers have become interested in FOCPs and time delay FOCPs in chemistry.

FOCPs and time delay FOCPs extend the classical integer-order models by adding nonlocal dynamics and memory effects. These effects are common in chemical processes because of factors like transport phenomena, diffusion, adsorption and desorption reactions, and complicated reaction steps.

In chemical engineering, these problems can create better models of reactors, distillation columns, heat exchangers, and catalytic beds, enabling improved stability, robustness, and performance with potentially reduced energy and material costs [33].

Enzymes, as efficient biocatalysts, regulate the reaction dynamics through substrate binding and cooperative effects. To better capture the memory-dependent nature of these processes and to maximize product yield and enhance system performance, a FOCP was formulated for the enzyme-kinetic model [34].

FOCPs have also been used in biomedical chemistry, especially for creating better chemotherapy dosing plans. The use of fractional and delay elements helps account for the body's memory effects and the delayed effect of drugs, which makes the treatment plans more effective and safer [35]. In addition, several examples of these applications are given in Table 1.

Table 1: Some applications of FOCPs in Chemistry.

Application/Phenomenon	Ref.
Chaotic chemical reaction model	Wang (2022) [36]
Fractional convection-diffusion-reaction system	Mahmoudi et al. (2023) [37]
Lithium-ion battery modeling	Zhang et al. (2023)[38]
Cancer treatment with fractional derivative	Sweilam et al. (2020) [39]

In this study, we address the following problem [31]:

$$\min \mathcal{J} = \mathcal{X}^T(1)\tilde{\mathcal{Q}}(1)\mathcal{X}(1) + \int_0^1 L(t, \mathcal{X}(t), \mathcal{U}(t))\mathrm{d}t, \tag{1}$$

Problem 1: subject to the establishment of the fractional system outlined below:

$$\mathcal{D}^\gamma \mathcal{X}(t) = \mathcal{A}(t)\mathcal{X}(t) + \mathcal{U}(t), \quad 0 \leq \gamma \leq 1, \tag{2}$$

and

$$\mathcal{X}(0) = \beta. \tag{3}$$

Problem 2: subject to the establishment of the delay fractional system outlined below:

$$\begin{cases} \mathcal{D}^\gamma \mathcal{X}(t) = \mathcal{A}(t)\mathcal{X}(t) + \mathcal{B}(t)\mathcal{X}(t-\varsigma) + \mathcal{U}(t), \quad t \in [0,1], \\ \mathcal{X}(0) = \beta, \\ \mathcal{X}(t) = \theta(t), \quad t \in [-\varsigma, 0). \end{cases} \tag{4}$$

subject to $\mathcal{X}(t) \in R^l$, $\mathcal{U}(t) \in R^q$, $(with\ l \geq q)$ $\mathcal{A}(t), \mathcal{B}(t)$, are continuous matrices with suitable dimensions, β is a constant vector, and $\theta_1(t)$ is a known function defined on the interval $[-\varsigma, 0)$. In both cases, $\mathcal{D}^\gamma$ denotes the Caputo fractional derivative as proposed in [40].

The general Lagrange scaling function provides a powerful approach for solving various fractional problems, because of its flexibility, ease of implementation, and efficiency. These functions feature a set of nodes that serve as free parameters for constructing both orthogonal and non-orthogonal Lagrange scaling functions [41]. Our proposed strategy in this study is based on these properties. In addition, we introduce two general operational matrices: the Riemann-Liouville and delay matrices. These matrices are formulated broadly, without fixing values for the free parameters. Notably, the delay operational matrix is presented in the exact form. The way these matrices are constructed significantly influences the accuracy of the proposed scheme.

This manuscript is structured as follows: Section 2 covers the essential concepts and tools. Section 3 outlines the development of the numerical method. Section 4 examines the convergence of the approximation. In Section 5, numerical experiments are conducted to verify the proposed approach. At long last, Section 6 summarizes the main concluding remarks.

2 GLSFs and their properties

Here, we provide a brief overview of the GLSFs and introduce a general Riemann-Liouville operational matrix for GLSFs.

2.1 GLSFs

GLSFs are defined based on a set of nodal points $t_i,\ i = 0, 1, \ldots, n$ within $[0, 1)$. These nodal points play a critical role in defining the general Lagrange scaling functions as described in the reference [40]:

$$\psi_{n,m}(t) = \begin{cases} 2^{\frac{\mathcal{K}-1}{2}} \tilde{\mathcal{L}}_m(2^{\mathcal{K}-1}t - n + 1), & t \in [\frac{n-1}{2^{\mathcal{K}-1}}, \frac{n}{2^{\mathcal{K}-1}}), \\ 0, & otherwise, \end{cases} \tag{5}$$

where

$$\tilde{\mathcal{L}}_m(t) = \frac{1}{\sqrt{\omega_m}} \mathcal{L}_m(t). \tag{6}$$

Also, $n = 1, 2, \ldots, 2^{\mathcal{K}-1}$, ω_m are determined in [40], and $\mathcal{L}_m(t),\ m = 0, \ldots, M-1$ are the Lagrange polynomials, which can be formulated as follows [40]:

$$\mathcal{L}_m(t) = \sum_{s=0}^{M-1} \zeta_{is} t^{M-1-s}, \tag{7}$$

where

$$\zeta_{m0} = \frac{1}{\prod_{\substack{j=0 \\ j \neq m}}^{M-1} (x_m - x_j)},$$

$$\zeta_{ms} = \frac{(-1)^s}{\prod_{\substack{j=0 \\ j \neq m}}^{M-1} (x_m - x_j)} \sum_{k_s = k_{s-1}+1}^{M-1} \cdots \sum_{k_1=0}^{M-s} \prod_{r=1}^{s} x_{k_r},$$

and $i \neq k_1 \neq \ldots \neq k_s,\ s = 1, 2, \ldots, M-1$.

2.2 GR-LOP of GLSFs

In the current part, we introduce a GR-LOP for GLSFs without explicit consideration of the Lagrange nodal points.

As the first step, we can express GLSFs, as shown in Eq. (5), in an alternative form as:

$$\psi_{n,m}(t) = 2^{\frac{\mathcal{K}-1}{2}} \tilde{\mathcal{L}}_m(2^{\mathcal{K}-1}t - n + 1) \chi_{[\frac{n-1}{2^{\mathcal{K}-1}}, \frac{n}{2^{\mathcal{K}-1}})}(t), \tag{8}$$

in which $\chi_{[\frac{n-1}{2^{\mathcal{K}-1}}, \frac{n}{2^{\mathcal{K}-1}})}(t)$ is the characteristic function. We consider

$$\begin{aligned} \Psi(t) &= [\psi_{1,0}(t), \ldots, \psi_{1,M-1}(t), \ldots, \psi_{2^{\mathcal{K}-1},0}(t), \ldots, \psi_{2^{\mathcal{K}-1},M-1}(t)]^T \\ &= [\psi_0(t), \psi_1(t), \ldots, \psi_{2^{\mathcal{K}-1}M-1}(t)]^T. \end{aligned} \tag{9}$$

Now, we can obtain the GR-LOP of GLSFs utilizing the expression provided in Equation (8) along with Equation (9) in the following form:

$$I^{\gamma} \Psi(t) \simeq \mathcal{P}_{\gamma} \Psi(t). \tag{10}$$

Let $\psi_{n,m}(t)$ be a component of $\Psi(t)$ in Equation (9). Based on Equations (5)-(8), we get

$$\psi_{n,m}(t) = 2^{\frac{\mathcal{K}-1}{2}} \tilde{\mathcal{L}}_m(2^{\mathcal{K}-1}t - n + 1) \chi_{[\frac{n-1}{2^{\mathcal{K}-1}}, \frac{n}{2^{\mathcal{K}-1}})}(t) \tag{11}$$

$$= \frac{2^{\frac{\mathcal{K}-1}{2}}}{\sqrt{\omega_m}} \sum_{s=0}^{M-1} \zeta_{ms} (2^{\mathcal{K}-1}t - n + 1)^{M-s-1} \chi_{[\frac{n-1}{2^{\mathcal{K}-1}}, \frac{n}{2^{\mathcal{K}-1}})}(t).$$

Subsequently, through the application of the binomial expansion of $(2^{\mathcal{K}-1}t - n + 1)^{M-s-1}$, the following relation is derived:

$$\psi_{n,m}(t) = \frac{2^{\frac{\mathcal{K}-1}{2}}}{\sqrt{\omega_m}} \sum_{s=0}^{M-1} \sum_{r=0}^{M-s-1} \zeta_{ms} \left(\begin{array}{c} M-s-1 \\ r \end{array} \right) 2^{(\mathcal{K}-1)r} t^r (1-n)^{M-s-1-r} \chi_{[\frac{n-1}{2^{\mathcal{K}-1}}, \frac{n}{2^{\mathcal{K}-1}})}(t).$$

Then, we obtain

$$\begin{aligned} I^\gamma \psi_{n,m}(t) &= \frac{2^{\frac{\mathcal{K}-1}{2}}}{\sqrt{\omega_m}} \sum_{s=0}^{M-1} \sum_{r=0}^{M-s-1} \zeta_{ms} \left(\begin{array}{c} M-s-1 \\ r \end{array} \right) 2^{(\mathcal{K}-1)r} (1-n)^{M-s-1-r} I^\gamma \left(t^r \chi_{[\frac{n-1}{2^{\mathcal{K}-1}}, \frac{n}{2^{\mathcal{K}-1}})}(t) \right) \\ &= \frac{2^{\frac{\mathcal{K}-1}{2}}}{\sqrt{\omega_m}} \sum_{s=0}^{M-1} \sum_{r=0}^{M-s-1} \zeta_{ms} \left(\begin{array}{c} M-s-1 \\ r \end{array} \right) 2^{(\mathcal{K}-1)r} (1-n)^{M-s-1-r} \varphi_r(t), \end{aligned} \tag{12}$$

where

$$\begin{aligned} \varphi_r(t) &= I^\gamma \left(t^r \chi_{[\frac{n-1}{2^{\mathcal{K}-1}}, \frac{n}{2^{\mathcal{K}-1}})}(t) \right) \\ &= \frac{1}{\Gamma(\gamma)} \int_{\frac{n-1}{2^{\mathcal{K}-1}}}^{t} \frac{\tau^r}{(t-\tau)^{1-\gamma}} \mathrm{d}\tau \chi_{[\frac{n-1}{2^{\mathcal{K}-1}}, \frac{n}{2^{\mathcal{K}-1}})}(t) \\ &+ \frac{1}{\Gamma(\gamma)} \int_{\frac{n-1}{2^{\mathcal{K}-1}}}^{\frac{n}{2^{\mathcal{K}-1}}} \frac{\tau^r}{(t-\tau)^{1-\gamma}} \mathrm{d}\tau \chi_{[\frac{n}{2^{\mathcal{K}-1}}, 1)}(t), \quad r = 0, 1, \cdots, M-s-1. \end{aligned}$$

Now, $\varphi_r(t), r = 0, 1, \cdots, M-s-1$, can be expanded via GLSFs as follows:

$$\varphi_r(t) \simeq \sum_{i=1}^{2^{k-1}} \sum_{j=0}^{M-1} \phi_{i,j} \psi_{i,j}(t).$$

Then, we derive

$$I^\gamma \psi_{n,m}(t) \simeq \sum_{i=1}^{2^{\mathcal{K}-1}} \sum_{j=0}^{M-1} \Phi_{i,j}^{n,m} \Psi_{i,j}(t),$$

in which

$$\Phi_{i,j}^{n,m} = \frac{2^{\frac{\mathcal{K}-1}{2}}}{\sqrt{\omega_m}} \sum_{s=0}^{M-1} \sum_{r=0}^{M-s-1} \zeta_{ms} \left(\begin{array}{c} M-s-1 \\ r \end{array} \right) 2^{(\mathcal{K}-1)r} (1-n)^{M-s-1-r} \phi_{i,j}.$$

Therefore, these coefficient vector $(\Phi^{n,m})$ are the rows of the mentioned operational matrix

$$\Phi^{n,m} = [\Phi_{1,0}^{n,m}, \cdots, \Phi_{1,M-1}^{n,m}, \cdots, \Phi_{2^{\mathcal{K}-1},0}^{n,m}, \cdots, \Phi_{2^{\mathcal{K}-1},M-1}^{n,m}]^T,$$

so, we have

$$\mathcal{P}_\gamma = [\Phi^{n,m}]. \tag{13}$$

2.3 GDOP of GLSFs

In this part, we obtain a GDOP of GLSFs. To achieve this, we define $\varsigma = \frac{s}{2^{\mathcal{K}-1}}$. Subsequently, we get

$$\Psi(t-\varsigma) = \mathcal{D}_{\varsigma}\Psi(t), \quad t > \varsigma. \tag{14}$$

Below, for each component of $\Psi(t-\varsigma)$, the following relation is established.

$$\begin{aligned}
\psi_{n,m}(t-\varsigma) &= \begin{cases} 2^{\frac{\mathcal{K}-1}{2}}\tilde{\mathcal{L}}_m(2^{\mathcal{K}-1}(t-\varsigma)-n+1), & t-\varsigma \in [\frac{n-1}{2^{\mathcal{K}-1}}, \frac{n}{2^{\mathcal{K}-1}}), \\ 0, & otherwise, \end{cases} \\
&= \begin{cases} 2^{\frac{\mathcal{K}-1}{2}}\tilde{\mathcal{L}}_m(2^{\mathcal{K}-1}(t-\frac{s}{2^{\mathcal{K}-1}})-n+1), & t-\frac{s}{2^{\mathcal{K}-1}} \in [\frac{n-1}{2^{\mathcal{K}-1}}, \frac{n}{2^{\mathcal{K}-1}}), \\ 0, & otherwise, \end{cases} \\
&= \begin{cases} 2^{\frac{\mathcal{K}-1}{2}}\tilde{\mathcal{L}}_m(2^{\mathcal{K}-1}t-(s+n)+1), & t \in [\frac{n-1+s}{2^{\mathcal{K}-1}}, \frac{n+s}{2^{\mathcal{K}-1}}), \\ 0, & otherwise, \end{cases} \\
&= \psi_{m,n+s}(t).
\end{aligned} \tag{15}$$

Hence, the GDOP of GLSFs ($\mathcal{D}_{\varsigma}$), in the order of $2^{\mathcal{K}-1}M \times 2^{\mathcal{K}-1}M$, is as:

$$\mathcal{D}_{\varsigma} = \begin{bmatrix} \mathbf{0} & \dots & \mathbf{0} & \mathrm{I} & \mathbf{0} & \dots & \mathbf{0} \\ \mathbf{0} & \dots & \mathbf{0} & \mathbf{0} & \mathrm{I} & \dots & \mathbf{0} \\ \vdots & \ddots & \vdots & \vdots & \vdots & \ddots & \vdots \\ \mathbf{0} & \dots & \mathbf{0} & \mathbf{0} & \mathbf{0} & \dots & \mathrm{I} \\ \mathbf{0} & \dots & \mathbf{0} & \mathbf{0} & \mathbf{0} & \dots & \mathbf{0} \\ \vdots & \ddots & \vdots & \vdots & \vdots & \ddots & \vdots \\ \mathbf{0} & \mathbf{0} & \dots & \mathbf{0} & \mathbf{0} & \dots & \mathbf{0} \end{bmatrix}, \tag{16}$$

in which ($\mathbf{0}$), and ($\mathbf{I}$) are the zero and identity matrices, respectively.

3 Approximation method

The main objective of this part is to introduce a computational technique based on the presented operational matrices for GLSFs, which were achieved in the previous section.

Step 1: Considering Equations (1)-(4), the relations in Equations (2) and (4) can be rewritten as:

Problem 1:

$$\mathcal{U}(t) = \mathcal{D}^{\gamma}\mathcal{X}(t) - \mathcal{A}(t)\mathcal{X}(t), \tag{17}$$

Problem 2:

$$\mathcal{U}(t) = \mathcal{D}^{\gamma}\mathcal{X}(t) - \mathcal{A}(t)\mathcal{X}(t) - \mathcal{B}(t)\mathcal{X}(t-\varsigma). \tag{18}$$

Step 2: Due to the GR-LOP, GDOP and the initial conditions, the unknown functions $\mathcal{X}(t)$ and $\mathcal{D}^{\gamma}\mathcal{X}(t)$ can approximated in the following form:

$$\mathcal{D}^{\gamma}\mathcal{X}(t) \simeq \hat{\mathcal{X}}(t) = X^T\Psi(t), \tag{19}$$

$$\mathcal{X}(t) \simeq \tilde{\mathcal{X}} = X^T\mathcal{P}_{\gamma}\Psi(t) + \mathcal{E}^T\Psi(t),$$

$$\mathcal{X}(t-\varsigma) \simeq \tilde{\mathcal{X}}(t-\varsigma) = \begin{cases} \theta(t-\varsigma), & 0 \le t \le \varsigma, \\ X^T\mathcal{P}_{\gamma}\mathcal{D}_{\varsigma}\Psi(t) + \mathcal{E}^T\mathcal{D}_{\varsigma}\Psi(t), & \varsigma \le t \le 1, \end{cases} \tag{20}$$

in which

$$\mathcal{X}(0) \simeq \mathcal{E}^T \Psi(t).$$

Step 3: According to the previous steps, we can obtain the unknown function $\mathcal{U}(t)$ in the following form:

Problem 1:

$$\mathcal{U}(t) \simeq X^T \Psi(t) - \mathcal{A}(t)(X^T \mathcal{P}_\gamma \Psi(t) + \mathcal{E}^T \Psi(t)) := \tilde{\mathcal{U}}(t), \tag{21}$$

Problem 2:

$$\mathcal{U}(t) \simeq X^T \Psi(t) - \mathcal{A}(t)\tilde{\mathcal{U}}(t-\varsigma) - \mathcal{B}(t)(X^T \mathcal{P}_\gamma \mathcal{D}_\varsigma \Psi(t)) := \hat{\mathcal{U}}(t). \tag{22}$$

Step 4: Substituting the approximations in Equations (19)-(22) into Equations (1)-(4), we obtain

Problem 1:

$$\tilde{\mathcal{J}} := \tilde{\mathcal{X}}^T(1)\tilde{\mathcal{Q}}(1)\tilde{\mathcal{X}}(1) + \int_0^1 L(t, \tilde{\mathcal{X}}(t), \tilde{\mathcal{U}}(t))\mathrm{d}t, \tag{23}$$

Problem 2:

$$\tilde{\mathcal{J}}^* := \tilde{\mathcal{X}}^T(1)\tilde{\mathcal{Q}}(1)\tilde{\mathcal{X}}(1) + \int_0^1 L(t, \tilde{\mathcal{X}}(t), \hat{\mathcal{U}}(t))\mathrm{d}t, \tag{24}$$

that we solve them approximately by the Gauss-Legendre integration approach, where $\mathcal{J} \simeq \tilde{\mathcal{J}}$, and $\mathcal{J} \simeq \tilde{\mathcal{J}}^*$. Then, the necessary conditions for deriving extremum are as:

Problem 1:

$$\frac{\partial \tilde{\mathcal{J}}}{\partial X} = 0, \tag{25}$$

Problem 2:

$$\frac{\partial \tilde{\mathcal{J}}^*}{\partial X} = 0. \tag{26}$$

Step 5: The unknown parameters can be computed by using "FindRoot" package in the Mathematica software. By replacing the approximations into Equations (19), (21)-(22), $\mathcal{X}(t)$ and $\mathcal{U}(t)$ in two problems can be computed.

4 Convergence of the GLSFs

In this section, to discuss the convergence of GLSFs, we refer to certain necessary tools outlined in reference [42]. Also, in [41], this discussion is proposed for the hybrid-Lagrange functions.

The Sobolev norm of integer-order $\varrho \geq 0$ and $|y|_{\mathcal{H}^{\varrho,M-1}(0,1)}$ are defined respectively by

$$\|y\|_{\mathcal{H}^\varrho(0,1)} = \left(\sum_{\iota=0}^{\varrho} \|y^{(\iota)}\|^2_{L^2(0,1)}\right)^{\frac{1}{2}}, \tag{27}$$

$$|y|_{\mathcal{H}^{\varrho,M-1}(0,1)} = \left(\sum_{\iota=\min(\varrho,M)}^{\varrho} \|y^{(\iota)}\|^2_{L^2(0,1)}\right)^{\frac{1}{2}}. \tag{28}$$

Also, for $y \in \mathcal{H}^\varrho(0,1), 0 \leq h \leq \varrho, M \geq 1, N \geq 1$, we consider the following seminorm

$$|y|_{\mathcal{H}^{\varrho,h;M-1,N}(0,1)} = \left(\sum_{\iota=\min(\varrho,M)}^{\varrho} N^{2h-2\iota}\|y^{(\iota)}\|^2_{L^2(0,1)}\right)^{\frac{1}{2}}. \tag{29}$$

and, we gain

$$|y|_{H^{h,\varrho;M-1,N}(0,1)} = N^{h-\varrho}\|y^{(\varrho)}\|_{L^2(0,1)}, \tag{30}$$

where, $M \geq \varrho - 1$.

Lemma 4.1. *Assume that $y \in \mathcal{H}^{\varrho}(0,1)$ and $Y_{M-1}(y) = \sum_{i=0}^{M-1} a_i \ell_i(t)$ is the best approximation for y. Thus, the truncation error $y - Y_{M-1}(y)$ is as [42]*

$$\|y - Y_{M-1}(y)\|_{L^2(0,1)} \leq \mathsf{c}(M-1)^{-\varrho}|y|_{\mathcal{H}^{\varrho,M-1}(0,1)}, \tag{31}$$

and, for $1 \leq h \leq \varrho$, we have

$$\|y - Y_{M-1}(y)\|_{\mathcal{H}^{h}(0,1)} \leq \mathsf{c}(M-1)^{\delta(h)-\varrho}|y|_{\mathcal{H}^{\varrho,M-1}(0,1)}, \tag{32}$$

subject to c depends on ϱ and, $\delta(h) = \begin{cases} 2h - \frac{1}{2}, & h > 0, \\ 0, & h = 0. \end{cases}$

Lemma 4.2. *Let $\mathsf{y}_n : (\frac{n-1}{2^{\mathcal{K}-1}}, \frac{n}{2^{\mathcal{K}-1}}) \to \mathcal{R}^2$ be a function in $\mathcal{H}^{\varrho}(\frac{n-1}{2^{\mathcal{K}-1}}, \frac{n}{2^{\mathcal{K}-1}}), n = 1, 2, \ldots, 2^{\mathcal{K}-1}$. For all $t \in (0,1)$, we consider $(F_n\mathsf{y}_n)(t) = \mathsf{y}_n(\frac{t}{2^{\mathcal{K}-1}} + \frac{n-1}{2^{\mathcal{K}-1}})$ which be a function as $F_n\mathsf{y}_n : (0,1) \to \mathcal{R}$. Then, for $0 \leq h \leq \varrho$, we get*

$$\|(F_n\mathsf{y}_n)^{(h)}\|_{L^2(0,1)} = 2^{(\mathcal{K}-1)(\frac{1}{2}-h)}\|\mathsf{y}_n^{(h)}\|_{L^2(\frac{n-1}{2^{\mathcal{K}-1}}, \frac{n}{2^{\mathcal{K}-1}})}. \tag{33}$$

Proof. Utilizing a change of variable $\tilde{t} = \frac{t}{2^{\mathcal{K}-1}} + \frac{n-1}{2^{\mathcal{K}-1}}$, we get

$$\begin{aligned} \|(F_n\mathsf{y}_n)^{(h)}\|^2_{L^2(0,1)} &= \int_0^1 |(F_n\mathsf{y}_n)^{(h)}(t)|^2 \mathrm{d}t = \int_0^1 |\mathsf{y}_n^{(h)}(\frac{t}{2^{\mathcal{K}-1}} + \frac{n-1}{2^{\mathcal{K}-1}})|^2 dt \\ &= \int_{\frac{n-1}{2^{\mathcal{K}-1}}}^{\frac{n}{2^{\mathcal{K}-1}}} 2^{(\mathcal{K}-1)(1-2h)}|\mathsf{y}_n^{(h)}(\tilde{t})|^2 \mathrm{d}\tilde{t} = 2^{(\mathcal{K}-1)(1-2h)}\|\mathsf{y}_n^{(h)}\|^2_{L^2(\frac{n-1}{2^{\mathcal{K}-1}}, \frac{n}{2^{\mathcal{K}-1}})}. \end{aligned}$$

In the aforesaid equation, the proof is completed by finding the square roots of both sides of the equation. ■

Theorem 4.3. *Let $y \in \mathcal{H}^{\varrho}(0,1), \varrho \geq 0$, then*

$$\|y - Y_{M-1}^{2^{\mathcal{K}-1}}(y)\|_{L^2(0,1)} \leq \frac{\mathsf{c}}{(M-1)^{\varrho}}|y|_{\mathcal{H}^{0,\varrho;M-1,2^{\mathcal{K}-1}}(0,1)}. \tag{34}$$

Moreover, for $1 \leq h \leq \varrho$, we get

$$\|y - Y_{M-1}^{2^{\mathcal{K}-1}}(y)\|_{\mathcal{H}^{h}(0,1)} \leq \mathsf{c}(M-1)^{\delta(h)-\varrho}|y|_{\mathcal{H}^{h,\varrho;M-1,2^{\mathcal{K}-1}}(0,1)}, \tag{35}$$

where $Y_{M-1}^{2^{\mathcal{K}-1}}(y) = \sum_{n=1}^{2^{\mathcal{K}-1}} \sum_{m=0}^{M-1} a_{n,m}\psi_{n,m}(t)$.

Proof. Consider the function $\mathsf{y}_n : (\frac{n-1}{2^{\mathcal{K}-1}}, \frac{n}{2^{\mathcal{K}-1}}) \to \mathcal{R}$, such that $\mathsf{y}_n(t) = y(t)$, where $n = 1, 2, \ldots, 2^{\mathcal{K}-1}$. Utilizing the concept of the Sobolev norm and the above lemmas, we have

$$\begin{aligned} \|y - Y_{M-1}^{2^{\mathcal{K}-1}}(y)\|^2_{L^2(0,1)} &= \sum_{n=1}^{2^{\mathcal{K}-1}} \|\mathsf{y}_n - \sum_{m=0}^{M-1} a_{n,m}\psi_{n,m}\|^2_{L^2(\frac{n-1}{2^{\mathcal{K}-1}}, \frac{n}{2^{\mathcal{K}-1}})} \\ &= 2^{-(\mathcal{K}-1)} \sum_{n=1}^{2^{\mathcal{K}-1}} \|(F_n\mathsf{y}_n) - (Y_{M-1}(F_n\mathsf{y}_n))\|^2_{L^2(0,1)} \end{aligned} \tag{36}$$

$$
\begin{aligned}
&\leq 2^{-(\mathcal{K}-1)}\frac{\mathsf{c}^2}{(M-1)^{2\varrho}}\sum_{n=1}^{2^{\mathcal{K}-1}}\sum_{i=\min\{\varrho,M\}}^{\varrho}\|(F_n\mathsf{y}_n)^{(i)}\|^2_{L^2(0,1)}\\
&= 2^{-(\mathcal{K}-1)}\frac{\mathsf{c}^2}{(M-1)^{2\varrho}}\sum_{i=\min\{\varrho,M\}}^{\varrho}\sum_{n=1}^{2^{\mathcal{K}-1}}(2^{\mathcal{K}-1})^{1-2i}\|(\mathsf{y}_n)^{(i)}\|^2_{L^2(\frac{n-1}{2^{\mathcal{K}-1}},\frac{n}{2^{\mathcal{K}-1}})}\\
&= \frac{\mathsf{c}^2}{(M-1)^{2\varrho}}\Big(\sum_{i=\min\{\varrho,M\}}^{\varrho}(2^{\mathcal{K}-1})^{-2i}\Big)\Big(\sum_{n=1}^{2^{\mathcal{K}-1}}\|(\mathsf{y}_n)^{(i)}\|^2_{L^2(\frac{n-1}{2^{\mathcal{K}-1}},\frac{n}{2^{\mathcal{K}-1}})}\Big)\\
&\leq \frac{\mathsf{c}^2}{(M-1)^{2\varrho}}|y|^2_{\mathcal{H}^{0,\varrho;M-1,2^{\mathcal{K}-1}}(0,1)}.
\end{aligned}
$$

For $1\leq h\leq\varrho$, we have

$$
\begin{aligned}
\|y-Y^{2^{\mathcal{K}-1}}_{M-1}(y)\|^2_{\mathcal{H}^h(0,1)} &= \sum_{n=1}^{2^{\mathcal{K}-1}}\|\mathsf{y}_n-\sum_{m=0}^{M-1}a_{n,m}\psi_{n,m}\|^2_{\mathcal{H}^h(\frac{n-1}{2^{\mathcal{K}-1}},\frac{n}{2^{\mathcal{K}-1}})}\\
&= \sum_{n=1}^{2^{\mathcal{K}-1}}\sum_{j=0}^{h}\|(\mathsf{y}_n)^{(j)}-\Big(\sum_{m=0}^{M-1}a_{n,m}\psi_{n,m}\Big)^{(j)}\|^2_{L^2(\frac{n-1}{2^{\mathcal{K}-1}},\frac{n}{2^{\mathcal{K}-1}})}\\
&= \sum_{n=1}^{2^{\mathcal{K}-1}}\sum_{j=0}^{h}(2^{\mathcal{K}-1})^{2j-1}\|(F_n\mathsf{y}_n)^{(i)}-(Y_{M-1}(F_n\mathsf{y}_n))^{(i)}\|^2_{L^2(0,1)}\\
&\leq \sum_{n=1}^{2^{\mathcal{K}-1}}(2^{\mathcal{K}-1})^{2h-1}\|(F_n\mathsf{y}_n)-Y_{M-1}(F_n\mathsf{y}_n)\|^2_{\mathcal{H}^h(0,1)}\\
&\leq \sum_{n=1}^{2^{\mathcal{K}-1}}(2^{\mathcal{K}-1})^{2h-1}\mathsf{c}^2(M-1)^{2\delta(h)-2\varrho}|F_n\mathsf{y}_n|^2_{H^{\varrho;M-1}(0,1)}\\
&= \sum_{n=1}^{2^{\mathcal{K}-1}}(2^{\mathcal{K}-1})^{2h-1}\mathsf{c}^2(M-1)^{2\delta(h)-2\varrho}\sum_{i=\min\{\varrho,M\}}^{\varrho}\|(F_n\mathsf{y}_n)^{(i)}\|^2_{L^2(0,1)}\\
&= (2^{\mathcal{K}-1})^{2h-1}\mathsf{c}^2(M-1)^{2\delta(h)-2\varrho}\sum_{i=\min\{\varrho,M\}}^{\varrho}\sum_{n=1}^{2^{\mathcal{K}-1}}(2^{\mathcal{K}-1})^{1-2i}\|(F_n\mathsf{y}_n)^{(i)}\|^2_{L^2(\frac{n-1}{2^{\mathcal{K}-1}},\frac{n}{2^{\mathcal{K}-1}})}\\
&= \mathsf{c}^2(M-1)^{2\delta(h)-2\varrho}\Big(\sum_{i=\min\{\varrho,M\}}^{\varrho}(2^{\mathcal{K}-1})^{2h-2i}\Big)\Big(\sum_{n=1}^{2^{\mathcal{K}-1}}\|(F_n\mathsf{y}_n)^{(i)}\|^2_{L^2(\frac{n-1}{2^{\mathcal{K}-1}},\frac{n}{2^{\mathcal{K}-1}})}\Big)\\
&\leq \mathsf{c}^2(M-1)^{2\delta(h)-2\varrho}\Big(\sum_{i=\min\{\varrho,M\}}^{\varrho}(2^{\mathcal{K}-1})^{2h-2i}\Big)\|(F_n\mathsf{y}_n)^{(i)}\|^2_{L^2(0,1)}\\
&= \mathsf{c}^2(M-1)^{2\delta(h)-2\varrho}|y|^2_{\mathcal{H}^{h,\varrho;M-1,2^{\mathcal{K}-1}}}.
\end{aligned}
$$

■

Table 2: The approximated solution obtained through the current method for the parameters $\mathcal{K} = 1$, $\mathcal{M} = 6$, and various values of γ (Sample 5.1).

γ	$\gamma = 1$	$\gamma = 0.95$	$\gamma = 0.85$	$\gamma = 0.75$	$\gamma = 0.65$
$\mathcal{J}$	0.3807970779778447	0.37380176519986513	0.35953251308912976	0.3450670306805795	0.330630872886888

Table 3: A Comparison of the approximated values of functional $\mathcal{J}$ for $\gamma = 1$ (Sample 5.1).

Methods	J
Chebyshev finite difference method [45]($m = 7$)	0.380797
Boubaker polynomials method [32]($m = 5$)	0.380797
Bernoulli wavelets method [43] ($\mathcal{K} = 1, \mathcal{M} = 4$)	0.380797
Fibonacci wavelets method [44]($\mathcal{K} = 1, \mathcal{M} = 4$)	0.380797070
Fibonacci wavelets method [44] ($\mathcal{K} = 2, \mathcal{M} = 4$)	0.380797079
Fibonacci wavelets method [44] ($\mathcal{K} = 3, \mathcal{M} = 4$)	0.380797078
Our scheme ($\mathcal{K} = 1, \mathcal{M} = 4$)	0.380797069466688
Our scheme ($\mathcal{K} = 2, \mathcal{M} = 4$)	0.380797077945354
Our scheme ($\mathcal{K} = 1, \mathcal{M} = 6$)	0.3807970779778447
Our scheme ($\mathcal{K} = 2, \mathcal{M} = 6$)	0.3807970779778821
Exact value	0.3807970779778824

5 Computational results

This section demonstrates the precision, effectiveness, and efficiency of the suggested approach using several numerical experiments. All numerical results were performed using Mathematica 12.0 software on a personal computer with 2.67-GHz Core i5.

Sample 5.1. Consider the FOCP below [43, 44]:

$$\mathcal{J} = \int_0^1 [0.625\mathcal{X}^2(t) + 0.5\mathcal{X}(t)\mathcal{U}(t) + 0.5\mathcal{U}^2(t)]\mathrm{d}t,$$

where

$$\mathcal{D}^{\gamma}\mathcal{X}(t) = 0.5\mathcal{X}(t) + \mathcal{U}(t),$$

and $\mathcal{X}(0) = 1$. The analytic solution to this example when $\gamma = 1$ can be found in [43]. This problem has been solved using various methods, including the Chebyshev finite difference method [45], the Boubaker polynomials method [32], the Bernoulli wavelets method [43], and the Fibonacci wavelets method [44]. We solve this problem by implementing the method described in the previous section, for some values of γ and $\mathcal{K} = 1, \mathcal{M} = 6$, and the results are listed in Table 2. Table 3 compares the optimal performance index $\mathcal{J}$ obtained through some existing methods. Figure 1 illustrates the characteristics of the approximate solutions of $\mathcal{X}(t)$ and $\mathcal{U}(t)$, under the conditions where $\mathcal{K} = 1$, $\mathcal{M} = 6$, across various values of γ. The findings highlight the superiority of the accuracy of the method that we have presented.

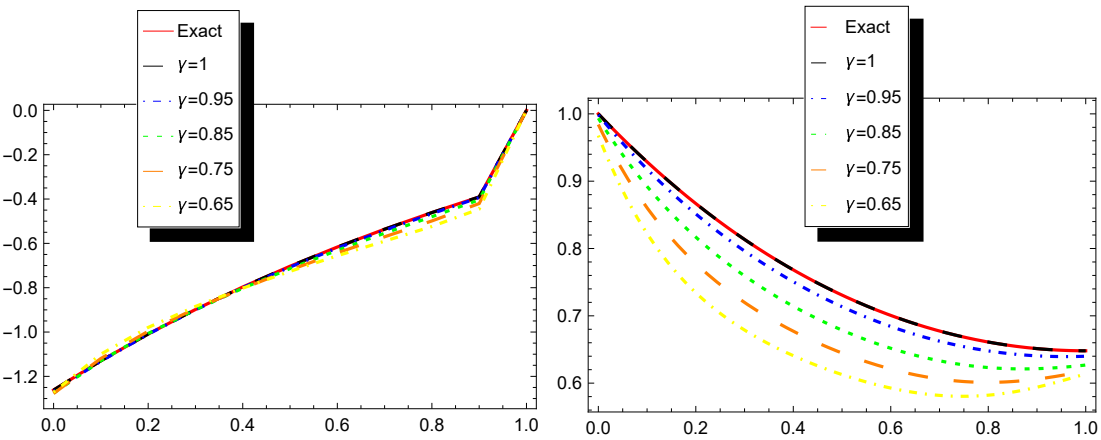

Figure 1: The plot of the approximate solutions for $\mathcal{U}(t)$ (left) and $\mathcal{X}(t)$ (right) with parameters $\mathcal{K} = 1$ and $\mathcal{M} = 6$, across a range of different values of γ (Sample 5.1).

Sample 5.2. Consider the FOCP below [46]:

$$\mathcal{J} = \frac{1}{2}\int_0^1 [\mathcal{X}^2(t) + \mathcal{U}^2(t)]\mathrm{d}t,$$

where

$$\mathcal{D}^\gamma \mathcal{X}(t) = -\mathcal{X}(t) + \mathcal{U}(t),$$

and $\mathcal{X}(0) = 1$.

For $\gamma = 1$, the analytic solutions in this example were proposed in a previous study by Agarwal [46]. The minimization of $\mathcal{J}$ yielded $\mathcal{J} = 0.192909298093169$. Implementing the algorithm discussed in Section 4 in some choices of $\mathcal{K}$ and $\mathcal{M}$ for $\gamma = 1$, we could solve the problem. A comparison between the numerical results achieved by the proposed methods for different values of $\mathcal{K}, \mathcal{M}$ and the value of $\mathcal{J}$ is tabulated in Table 4. Figure 2 displays the behavior of the approximate solutions in some choices of γ. In addition, Figure 3 shows the absolute error functions when $\gamma = 1$ and $\mathcal{K} = 2, \mathcal{M} = 6$ for $\mathcal{X}(t)$, and $\mathcal{U}(t)$. The results indicate that the approximated solutions closely match the analytic solutions for the case $\gamma = 1$.

Sample 5.3. We consider the following problem

$$\mathcal{J} = \frac{1}{2}\int_0^1 [\mathcal{X}^2(t) + \mathcal{U}^2(t)]\mathrm{d}t.$$

where

$$\mathcal{D}^\gamma \mathcal{X}(t) = t\mathcal{X}(t) + \mathcal{U}(t),$$

and $\mathcal{X}(0) = 1$. To solve the problem, we apply the present technique with different values of $\mathcal{K}, \mathcal{M}$ and γ. In Table 5, we list the approximate results of $\mathcal{J}$ for the method and the Boubacker polynomials method [32] ($m = 4$, or 5 basis function) and the Bernoulli polynomials method [49] ($m = 5$ or 5 basis function) in some values of γ.

Sample 5.4. We consider the following FDOCP [50]:

$$\mathcal{J} = \int_0^1 [\mathcal{X}^2(t) + \mathcal{U}^2(t)]\mathrm{d}t,$$

Table 4: A comparison of the approximated values of functional $\mathcal{J}$ for $\gamma = 1$ (Sample 5.2).

Methods	$\mathcal{J}$
Epsilon-Ritz method [47] ($N = 8$)	0.192909
Bessel collocation method [48] ($n = 5$)	0.1929065847
Fibonacci wavelets method [44]($\mathcal{K} = 1, \mathcal{M} = 4$)	0.192909275
Our scheme ($\mathcal{K} = 1, \mathcal{M} = 4$)	0.192909271553861
Our scheme ($\mathcal{K} = 2, \mathcal{M} = 4$)	0.192909297993919
Our scheme ($\mathcal{K} = 1, \mathcal{M} = 6$)	0.192909298092712
Our scheme ($\mathcal{K} = 2, \mathcal{M} = 6$)	0.192909298093168
Exact value	0.192909298093169

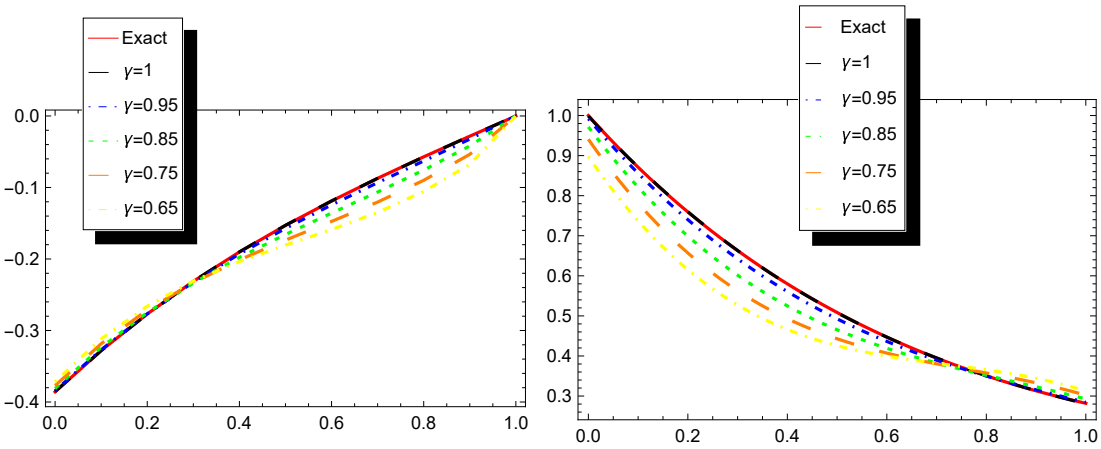

Figure 2: The plot of approximate solutions for the approximate of $\mathcal{U}(t)$ (left) and $\mathcal{X}(t)$ (right) with $\mathcal{K} = 1, \mathcal{M} = 4$, in different values of γ (Sample 5.2).

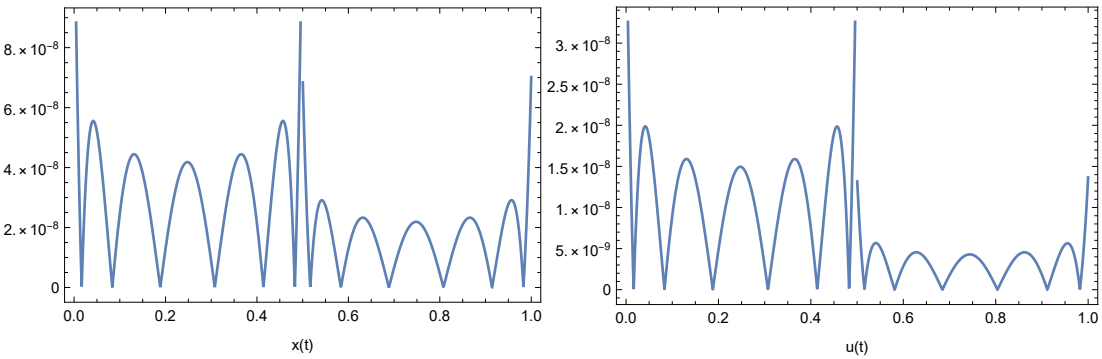

Figure 3: The absolute error functions for $\mathcal{X}(t)$ (left) and $\mathcal{U}(t)$ (right) in $\gamma = 1$ (Sample 5.2).

Table 5: The solution achieved via the proposed technique for some values of γ (Sample 5.3).

γ	Bernoulli polynomials method [49] $m=5$	Boubacker polynomials method [32] $m=4$	Proposed scheme $\mathcal{K}=1,\mathcal{M}=5$	Proposed scheme $\mathcal{K}=2,\mathcal{M}=5$	Proposed scheme $\mathcal{K}=2,\mathcal{M}=6$
1	0.484268	0.484268	0.484267753	0.484267696	0.484267696
0.99	0.483463	0.483463	0.483462738	0.483462653	0.483462653
0.9	0.475883	0.476024	0.475883175	0.475882669	0.475882669
0.8	0.466978	0.467669	0.466979407	0.466977787	0.466977787

Table 6: A comparison of the approximated values of functional $\mathcal{J}$ for $\gamma=1$ (Sample 5.4).

Methods	J
AAm [53]	1.6419
WFm [52]	1.6497
linear programming [51]	1.64886527
Our scheme ($\mathcal{K}=2,\mathcal{M}=4$)	1.6478743115
Our scheme ($\mathcal{K}=2,\mathcal{M}=6$)	1.6478741928

where

$$\mathcal{D}^{\gamma}\mathcal{X}(t)=2\mathcal{X}(t-\frac{1}{2})+2\mathcal{U}(t),\quad 0\leq t\leq 1,$$

and $\mathcal{X}(t)=1,\quad -\frac{1}{2}\leq t\leq 0$. For $\gamma=1$, the approximate values of $\mathcal{J}$ are proposed by applying some numerical methods such as linear programming [51], Walsh function (WFm) [52], and the averaging approximation (AAm) [53]. Table 6 reports these and presents a comparison with the numerical solution of our method. In addition, we solve this sample utilizing the scheme and we report the derived results for some values of γ and $\mathcal{K}=2,\mathcal{M}=4$ in Table 7.

Sample 5.5. Consider the FDOCP below [50]:

$$\mathcal{J}=\frac{3}{2}\mathcal{X}^2(t)+\frac{1}{2}\int_0^2\mathcal{U}^2(t)\mathrm{d}t,$$

where

$$\begin{cases}\mathcal{D}^{\gamma}\mathcal{X}(t)=\mathcal{X}(t)+\mathcal{X}(t-1)+\mathcal{U}(t), & 0\leq t\leq 2,\\ \mathcal{X}(t)=1, & -1\leq t\leq 0.\end{cases}$$

For $\gamma=1$, the analytic solution for $\mathcal{U}(t)$ is

$$\mathcal{U}(t)=\begin{cases}\delta(e^{2-t}+(1-t)e^{1-t}), & 0\leq t\leq 1,\\ \delta e^{2-t}, & 1\leq t\leq 2.\end{cases}$$

where $\delta=-0.3932$, $\mathcal{J}\simeq 3.1017$. The current method solved this problem as well. A study was conducted comparing the numerical outcomes obtained from the suggested approach, AAm

Table 7: The approximate solution achieved using our scheme for $\mathcal{K}=2,\mathcal{M}=4$ and some values of γ (Sample 5.4).

γ	$\gamma=1$	$\gamma=0.95$	$\gamma=0.85$	$\gamma=0.75$	$\gamma=0.65$
$\mathcal{J}$	1.647874	1.637539	1.609902	1.573297	1.529131

Table 8: Comparison of the approximated value of functional $\mathcal{J}$, with some methods (Sample 5.5).

Numerical methods	$\mathcal{J}$
AAm [53]	3.0833
WFm [52]	3.0879
VIm [54]	3.1091
Our scheme ($\mathcal{K}=3,\mathcal{M}=4$)	3.10026
Our scheme ($\mathcal{K}=3,\mathcal{M}=6$)	3.10058
Exact value	3.1017

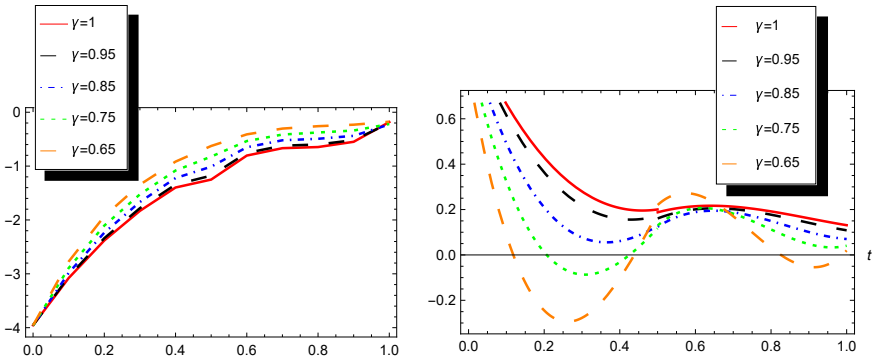

Figure 4: The plot approximate solutions for approximate $\mathcal{U}(t)$ (left) and $\mathcal{X}(t)$ (right) with $\mathcal{K}=2,\mathcal{M}=4$, in different values of γ (Sample 5.5).

[53], WFm [52], and variational iteration method (VIm) [54] for $\gamma=1$. Table 8 compares the optimal performance index $\mathcal{J}$ obtained through some existing methods. In addition, the figures depicting the numerical solutions for $\mathcal{K}=2,\mathcal{M}=4$ and various fractional-order γ selections are presented in Figure 4.

6 Conclusion

The current manuscript examined two classes of FOCPs. The general Lagrange scaling functions, as a suitable class of basis functions, were explored to deal with the problems. A new general Riemann-Liouville operational matrix and delay operational matrix were achieved for GLSFs. The general Lagrange scaling functions were used to develop two computational techniques for solving the considered problems. More precisely, the present techniques have applied GLSFs and their general operational matrices to reduce solving the problems to solving algebraic systems. To demonstrate the efficiency and effectiveness of the proposed schemes, some tests were conducted. The reported approximate results were compared with the exact solutions and the numerical results obtained by some existing schemes. Considering the advantages of GLSFs, the proposed framework can be extended to design flexible numerical schemes by selecting different nodal points. This flexibility may facilitate the solution of various fractional problems, including FOCPs involving fractal and piecewise fractional derivatives, and can be

considered as future work.

Conflicts of Interest. The authors declare that they have no conflicts of interest regarding the publication of this article.

Acknowledgments. The authors thank the editor and the anonymous reviewers for their helpful comments and suggestions that greatly improved the manuscript.

References

[1] R. Hilfer, *Applications of Fractional Calculus to Physics*, World Scientific, 2000.

[2] T. M. Atanackovic, S. Pilipovic, B. Stankovic and D. Zorica, *Fractional Calculus with Applications in Mechanics*, Wiley, London, 2014.

[3] N. Engheta, On fractional calculus and fractional multipoles in electromagnetism, *IEEE Trans. Antennas Propag.* **44** (1996) 554–566, https://doi.org/10.1109/8.489308.

[4] K. B. Oldham, Fractional differential equations in electrochemistry, *Adv. Eng. Softw.* **41** (2010) 9–12, https://doi.org/10.1016/j.advengsoft.2008.12.012.

[5] F. Mainardi, *Fractional Calculus: Some Basic Problems in Continuum and Statistical Mechanics*, Springer Verlag, New York, 1997.

[6] F. C. Meral, T. J. Royston and R. Magin, Fractional calculus in viscoelasticity: An experimental study, *Commun. Nonlinear Sci. Numer. Simul.* **15** (2010) 939–945, https://doi.org/10.1016/j.cnsns.2009.05.004.

[7] A. H. Ganie, M. Houas and M. E. Samei, Pantograph system with mixed Riemann-Liouville and Caputo-Hadamard sequential fractional derivatives: existence and Ulam-stability, *Math. Interdisc. Res.* **10** (2025) 1–33, https://doi.org/10.22052/MIR.2024.254075.1453

[8] G. H. Askarirobati, A. Hashemi Borzabadi and A. Heydari, Solving multi-objective optimal control problems of chemical processes using hybrid evolutionary algorithm, *Iranian J. Math. Chem.* **10** (2019) 103–126, https://doi.org/10.22052/IJMC.2018.137247.1370.

[9] P. Agarwal, J. Tariboon and S. K. Ntouyas, Some generalized Riemann-Liouville k-fractional integral inequalities, *J. Inequal. Appl.* **2016** (2016) #122, https://doi.org/10.1186/s13660-016-1067-3.

[10] A. A. El-Sayed, D. Baleanu and P. Agarwal, A novel Jacobi operational matrix for numerical solution of multi-term variable-order fractional differential equations, *J. Taibah Univ. Sci.* **14** (2020) 963–974, https://doi.org/10.1080/16583655.2020.1792681.

[11] P. Agarwal, A. A. El-Sayed and J. Tariboon, Vieta-Fibonacci operational matrices for spectral solutions of variable-order fractional integro-differential equations, *J. Comput. Appl. Math.* **382** (2021) #113063, https://doi.org/10.1016/j.cam.2020.113063.

[12] S. Sabermahani, P. Rahimkhani and Y. Ordokhani, Pell wavelet-optimization procedure for two classes of fractional partial differential equations with nonlocal boundary conditions, *J. Comput. Sci.* **90** (2025) #102655, https://doi.org/10.1016/j.jocs.2025.102655.

[13] G. Singh, P. Agarwal, M. Chand and S. Jain, Certain fractional kinetic equations involving generalized k-Bessel function, *Trans. A. Razmadze Math. Inst.* **172** (2018) 559–570, https://doi.org/10.1016/j.trmi.2018.03.001.

[14] X. Zhang, P. Agarwal, Z. Liu and H. Peng, The general solution for impulsive differential equations with Riemann-Liouville fractional-order $q \in (1, 2)$, *Open Mathematics* **13** (2015).

[15] G. Karamali and H. Mohammadi-Firouzjaei, The matrix Transformation technique for the time-space fractional linear Schrödinger equation, *Iranian J. Math. Chem.* **15** (2024) 137–154, https://doi.org/10.22052/IJMC.2024.254206.1812.

[16] M. H. Heydari and M. Razzaghi, Extended Chebyshev cardinal wavelets for nonlinear fractional delay optimal control problems, *Int. J. Syst. Sci.* **53** (2022) 1048–1067, https://doi.org/10.1080/00207721.2021.1987579.

[17] A. B. Salati, M. Shamsi and D. F. M. Torres, Direct transcription methods based on fractional integral approximation formulas for solving nonlinear fractional optimal control problems, *Commun. Nonlinear Sci. Numer. Simul.* **67** (2019) 334–350, https://doi.org/10.1016/j.cnsns.2018.05.011.

[18] E. Ashpazzadeh, M. Lakestani and A. Yildirim, Biorthogonal multiwavelets on the interval for solving multidimensional fractional optimal control problems with inequality constraint, *Optim. Control Appl. Methods.* **41** (2020) 1477–1494, https://doi.org/10.1002/oca.2615.

[19] H. R. Marzban and F. Malakoutikhah, Solution of delay fractional optimal control problems using a hybrid of block-pulse functions and orthonormal Taylor polynomials, *J. Frankl. Inst.* **356** (2019) 8182–8215, https://doi.org/10.1016/j.jfranklin.2019.07.010.

[20] N. Kumar and M. Mehra, Collocation method for solving nonlinear fractional optimal control problems by using Hermite scaling function with error estimates, *Optimal Control Appl. Methods* **42** (2021) 417–444, https://doi.org/10.1002/oca.2681.

[21] M. H. Heydari, A direct method based on the Chebyshev polynomials for a new class of nonlinear variable-order fractional 2D optimal control problems, *J. Franklin Inst.* **356** (2019) 8216–8236, https://doi.org/10.1016/j.jfranklin.2019.07.012.

[22] A. Ghasempour, Y. Ordokhani and S. Sabermahani, Mittag-Leffler wavelets and their applications for solving fractional optimal control problems, *J. Vib. Control* **31** (2025) 753–767, https://doi.org/10.1177/10775463241232178.

[23] H. Hassani, J. A. Tenreiro Machado, Z. Avazzadeh, E. Naraghirad and M. Sh. Dahaghin, Generalized Bernoulli polynomials: solving nonlinear 2D fractional optimal control problems, *J. Sci. Comput.* **83** (2020) #30.

[24] H. Hassani, M. Tenreiro, A. José, M. K. Hosseini Asl and M. Sh. Dahaghin, Numerical solution of nonlinear fractional optimal control problems using generalized Bernoulli polynomials *Optimal Control Appl. Methods* **42** (2021) 1045–1063, https://doi.org/10.1002/oca.2715.

[25] H. Hassani and Z. Avazzadeh, Novel operational matrices for solving 2-dim nonlinear variable order fractional optimal control problems via a new set of basis functions, *Appl. Numer. Math.* **166** (2021) 26–39, https://doi.org/10.1016/j.apnum.2021.03.015.

[26] Z. Avazzadeh, H. Hassani, A. Bayati Eshkaftaki, M. J. Ebadi and P. Agarwal, Optimal solution of nonlinear 2D variable-order fractional optimal control problems using generalized Bessel polynomials, *J. Vib. Control* **31** (2025) 1457–1471, https://doi.org/10.1177/10775463241227475.

[27] H. Hassani, Z. Avazzadeh, Z., J. A. Tenreiro Machado and E. Naraghirad, A new hybrid method for two dimensional nonlinear variable order fractional optimal control problems, *Asian J. Control* **23** (2021) 2004–2018, https://doi.org/10.1002/asjc.2351.

[28] H. R. Marzban, Numerical solution of optimal control problems governed by integro-differential equations, *Asian J. Control* **22** (2020) 1138–1146, https://doi.org/10.1002/asjc.1994.

[29] P. Rahimkhani, Y. Ordokhani and S. Sabermahani, An accurate wavelets-collocation technique for neutral delay distributed-order fractional optimal control problems, *Optimal Control Appl. Methods*, **46** (2025) 94–113, https://doi.org/10.1002/oca.3201.

[30] H. Hassani, J. A. Tenreiro Machado and E. Naraghirad, Generalized shifted Chebeshev polynomials for fractional optimal control problems, *Commun. Nonlinear Sci. Numer. Simul.* **75** (2019) 50–61, https://doi.org/10.1016/j.cnsns.2019.03.013.

[31] S. Sabermahani, Y. Ordokhani, S. A. Yousefi, Fractional-order Lagrange polynomials: an application for solving delay fractional optimal control problems, *Trans. Inst. Meas. Control.* **41** (2019) 2997–3009, https://doi.org/10.1177/0142331218819048.

[32] K. Rabiei, Y. Ordokhani and S. Babolian, The Boubaker polynomials and their application to solve fractional optimal control problems, *Nonlinear Dynam.* **88** (2017) 1013–1026, https://doi.org/10.1007/s11071-016-3291-2.

[33] R. Caponetto, G. Dongola, L. Fortuna and I. Petras, *Fractional Order Systems: Modeling and Control Applications*, World Scientific, 2010.

[34] F. Al-Basir, A. M. Elaiw, D. Kesh and P. K. Roy, Optimal control of a fractional-order enzyme kinetic model, *Control Cybernet.* **44** (2015) 443–461.

[35] N. Singha, Implementation of fractional optimal control problems in real-world applications, *Fract. Calc. Appl. Anal.* **23** (2020) 1783–1796, https://doi.org/10.1515/fca-2020-0088.

[36] H. Wang, Suppressing Chaos for a fractional-order chaotic chemical reaction model via PDζ controller, *J. Math.* 2022 #5658680.

[37] M. Mahmoudi, T. Shojaeizadeh and M. Darehmiraki, Optimal control of time-fractional convection-diffusion-reaction problem employing compact integrated RBF method, *Math. Sci.* **17** (2023) 1–14, https://doi.org/10.1007/s40096-021-00434-0.

[38] X. Zhang, X. Li, K. Yang and Z. Wang, Lithium-ion battery modeling and state of charge prediction based on fractional-order calculus, *Mathematics*, **11** (2023) #3401, https://doi.org/10.3390/math11153401.

[39] N. H. Sweilam, S. M. Al-Mekhlafi, T. Assiri and A. Atangana, Optimal control for cancer treatment mathematical model using Atangana-Baleanu-Caputo fractional derivative, *Adv. Difference Equ.* **2020** (2020) #334.

[40] S. Sabermahani, Y. Ordokhani and S. A. Yousefi, Fractional-order general Lagrange scaling functions and their applications, *BIT Numer. Math.* **60** (2020) 101–128, https://doi.org/10.1007/s10543-019-00769-0.

[41] H. R. Marzban and H. R.Tabrizidooz, Composite interpolation method and the corresponding differentiation matrix, *Bull. Iranian Math. Soc.* **37** (2011) 21–34.

[42] C. Canuto, M. Hussaini, A. Quarteroni and T. A. Zang, *Spectral Methods: Fundamentals in Single Domains*, Springer, Berlin, 2006.

[43] Z. Barikbin and E. Keshavarz, Solving fractional optimal control problems by new Bernoulli wavelets operational matrices, *Optimal Control Appl. Methods* **41** (2020) 1188–1210, https://doi.org/10.1002/oca.2598.

[44] S. Sabermahani and Y. Ordokhani, Fibonacci wavelets and Galerkin method to investigate fractional optimal control problems with bibliometric analysis, *J. Vib. Control.* **27** (2021) 1778–1792, https://doi.org/10.1177/1077546320948346.

[45] M. El-Kady, A Chebyshev finite difference method for solving a class of optimal control problems, *Int. J. Comput. Math.* **80** (2003) 883–895, https://doi.org/10.1080/0020716031000070625.

[46] O. P. Agrawal, General formulation for the numerical solution of optimal control problems, *Internat. J. Control* **50** (1989) 627–638, https://doi.org/10.1080/00207178908953385.

[47] A. Lotfi and S. A. Yousefi, Epsilon-Ritz method for solving a class of fractional constrained optimization problems, *J. Optim. Theory Appl.* **163** (2014) 884–899, https://doi.org/10.1007/s10957-013-0511-5.

[48] E. Tohidi and H. Saberi Nikv, A Bessel collocation method for solving fractional optimal control problems, *Appl. Math. Model.* **39** (2015) 455–465, https://doi.org/10.1016/j.apm.2014.06.003.

[49] E. Keshavarz, Y. Ordokhani and M. Razzaghi, A numerical solution for fractional optimal control problems via Bernoulli polynomials, *J. Vib. Control* **22** (2016) 3889–3903, https://doi.org/10.1177/1077546314567181.

[50] S. Sabermahani, Y. Ordokhani and S. A. Yousefi, Fibonacci wavelets and their applications for solving two classes of time-varying delay problems, *Optimal Control Appl. Methods* **41** (2020) 395–416, https://doi.org/10.1002/oca.2549.

[51] A. Jajarmi and D. Baleanu, Suboptimal control of fractional-order dynamic systems with delay argument, *J. Vib. Control* **24** (2018) 2430–2446, https://doi.org/10.1177/1077546316687936.

[52] K. R. Palanisamy and R. G. Prasada, Optimal control of linear systems with delays in state and control via Walsh functions, *IEE Proc. D (Control Theory and Applications)* **130** (1983) 300–312, https://doi.org/10.1049/ip-d.1983.0051.

[53] H. T. Banks and J. A. Burns, Hereditary control problems: numerical methods based on averaging approximations, *SIAM J. Control Optim.* **16** (1978) 169–208, https://doi.org/10.1137/0316013.

[54] S. M. Mirhosseini-Alizamini, S. Effati and A. Heydari, An iterative method for suboptimal control of linear time-delayed systems, *Systems Control Lett.* **82** (2015) 40–50.